Express Polymer Letters Vol.18, No.7 (2024) 705–714
Available online at www.expresspolymlett.com
https://doi.org/10.3144/expresspolymlett.2024.52

Research article

Toughness enhancement of polyamide 1012 with intermolecular hydrogen bonding with 3-pentadecylphenol

Jing Lu[1,2,3], *Qin Ma*[1,2], *Jianqi Yao*[1,2], *Jiajie Yin*[1,2], *Ruiyan Zhang*[1,2], *Faliang Luo*[1,2*]

[1]State Key Laboratory of High-efficiency Utilization of Coal and Green Chemical Engineering, Ningxia University, 750021 Yinchuan, China
[2]School of Chemistry and Chemical Engineering, Ningxia University, 750021 Yinchuan, China
[3]Gansu Province Building Materials Research and Design Institute co., ltd. Ningxia Branch, 750001 Yinchuan, China

Received 18 March 2024; accepted in revised form 23 April 2024

Abstract. In order to improve the impact toughness of polyamide 1012 (PA1012) by reducing the amount of hydrogen bonding resulting from PA1012 itself, 3-pentadecylphenol (PDP) was considered to be added into PA1012 using melting extrusion. The hydrogen bonding interaction between PA1012 and PDP was characterized by Fourier transform infrared spectroscopy (FTIR) and nuclear magnetic resonance (NMR). The effects of PDP on the crystallization, melting process, and mechanical behavior of PA1012 were tested in detail. The results show that the PDP can reduce the temperature of PA1012 crystallization and melting but it can significantly improve elongation at break and impact toughness. The notched impact strength of the PA1012/PDP composites containing 20 wt% PDP reached to 70.6 kJ·m^{-2}, which is about seven times that of the neat PA1012. The effects of PDP on PA1012 properties is ascribed to hydrogen bonding interaction between hydrogen bonding between phenol hydroxyl groups and amino groups on PA1012 chains. The deduction was also verified by adding acetylated 3-pentadecylphenol (APDP) to modify PA1012. It is believed the research will open up new prospects for the wide application of PA1012 toughening.

Keywords: *thermoplastic composites. additive. toughness. dynamic-mechanical analysis. mechanical properties*

1. Introduction

Polyamide 1012 (PA1012), as one of the most important bio-based thermoplastic engineering materials [1, 2], has attracted extensive attention in industrial application and academic research due to its superior properties, including lower water absorption, dimensional stability, excellent solvent resistance and high strength [3–5]. Unfortunately, PA1012 is highly sensitive to notch and presents brittle fracture behavior at severe loading conditions. Thus limit the application of PA1012 in the fields of automobiles and medical, *etc.* [6, 7]. So, improving the impact toughness of polyamide has been extensively focused on in recent years.

Blending elastomer [8] or rubber [9] into polyamide (PA) is a conventional strategy. For example, poly (octene-*co*-ethylene) [10] and ethylene propylene diene monomer [7] have been selected to toughen polyamide by forming crazing and shear yield bands. Moreover, some inorganic fillers, such as carbon nanotubes (CNTs) [11] and tetra-needle-shaped zinc oxide whiskers (T-ZnOw) [12], were proven to increase the impact toughness of PA. Nevertheless, complex surface modification becomes necessary because the nano-inorganic particle is difficult to disperse evenly in PA matrix [13]. In fact, it is different from other polymers that the strong hydrogen bonding within and between polyamide molecules is one

*Corresponding author, e-mail: flluo@iccas.ac.cn

important contributing factor to its low-impact toughness [14]. Reduction of the intramolecular and intermolecular hydrogen bonding of polyamide may improve its impact toughness. For instance, after the intermolecular interaction between polyamide 1010 (PA1010) and polyurethane is formed, the intramolecular hydrogen bonds interaction of PA1010 is reduced so that the impact strength of PA1010 is increased after the addition of polyurethane [15]. Incorporating small molecular compounds with some phenols and alcohol groups, can also form intermolecular hydrogen bonds with PA to improve its impact toughness [16]. As a compound of natural origin, 3-pentadecylphenol (PDP) has a phenol ring with one pentadecyl (C_{15}) chain, mainly exists in cashew nut shells and has a wide range of sources [17–19]. Intermolecular hydrogen bonds can form between the phenol hydroxyl group and the amide group of PA (Figure 1). In addition, the long chain alkyl of PDP can increase the free volume of PA molecular chain and form branched structure to plasticize to improve the impact toughness of PA. Our previous work on toughening of polyamide 612 (PA612) by PDP has confirmed the hypothesis. However, this hypothesis still requires more experimental evidence. Here, PA1012 was selected to toughen by PDP. In addition, acetylated PDP were used to further explore the significance of intermolecular hydrogen bond for PA1012 toughening.

2. Experimental

2.1. Materials

The density of 1030 kg·m^{-3} of PA1012 resin (B150) was bought from Shandong Guangyin New Material Co., Ltd. (China). PDP, a molecular weight of 304.52 (M_w = 304.52 g/mol, purity > 90%), was kindly supplied from Shanghai Chemical Industry Development Co., Ltd. (China). Dichloromethane (CH_2Cl_2, CAS:75-09-2) was purchased from Sinophosphoric Chemical Reagent Co., Ltd. (China), Triethylamine ($C_6H_{15}N$, CAS:121-44-8) was purchased from Shanghai Aladdin Biochemical Technology Co., Ltd. (China), acetyl chloride (C_2H_3ClO, CAS:75-36-5) was purchased from Shanghai McLean Biochemical Technology Co., Ltd. (China), Anhydrous sodium sulfate (Na_2SO_4, CAS:7757-82-6) acquired from Shanghai Aladdin Biochemical Technology Co., Ltd. (China).

2.2. Preparation of acetylated PDP (APDP)

In order to explore the toughening mechanism of PDP on PA1012, the phenol hydroxyl group in PDP was acetylated. The acetylation process is as follows. Firstly, 12.18 g of PDP was dissolved in redistilled dichloromethane with stirring, then 16.7 ml of triethylamine was added with a syringe. The reaction was carried out in an ice bath, and subsequently, 6.3 ml of acetyl chloride was added dropwise under magnetic stirring. After the reaction was complete, the sample was poured into a separating funnel and extracted with saturated NaCl. The extracts were dried and filtrated successively by sodium sulfate and vacuum filtration. The obtained sample was further purified through rotary evaporation and column chromatography separation. The schematic diagram of acetylation process for PDP is shown in Figure 2.

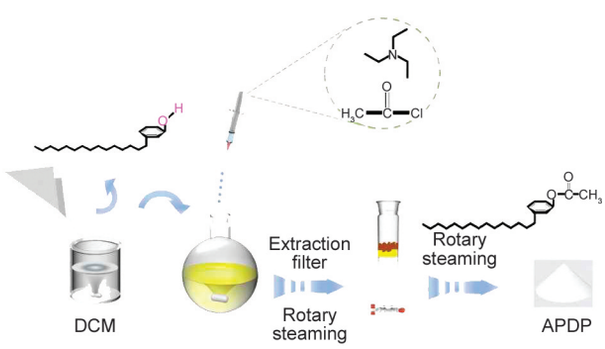

Figure 2. Synthetic route of acetylated PDP.

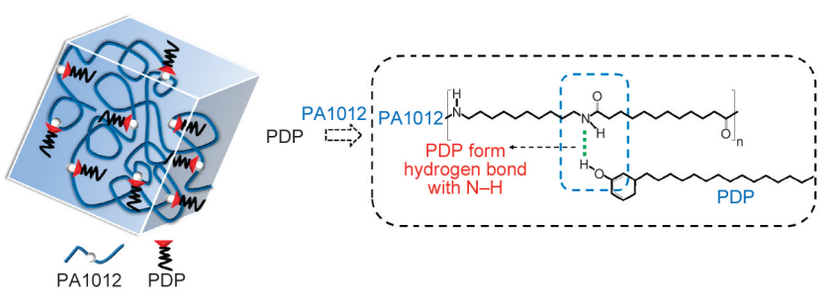

Figure 1. Schematic illustration of H-bonding formation between PA1012 and PDP molecular chains.

2.3. Preparation of PA1012/PDP composites

Prior to melt compounding, PA1012 pellets and PDP powder were dried at 85 and 40 °C overnight in a vacuum oven, respectively. Then, the PA1012/PDP and PA1012/APDP composites were prepared by a twin screw extruder (SJZS-10A, Wuhan Ruiming Experimental Instrument Manufacturing Co., Ltd., China) with an increasing temperature profile of 210–220 °C at a screw speed of 30 rpm. Then, the sample was shaped into dumbbell (75×5×2 mm) and rectangle (80×10×4 mm) form for corresponding mechanical property tests under 0.6 MPa and 225 °C by a micro injection molding machine. The PDP in the prepared composites are 5, 10, 20, 30 wt%, respectively, and APDP loading are 20 wt%.

2.4. Characterization methods

NMR spectroscopy was performed on the Bruker AVANCE III400 (Bruker, Switzerland) instrument using deuterated chloroform ($CDCl_3$) as solvent.

Fourier transform infrared spectroscopy (FTIR) (Spectrum Two, Perkin Elmer Instruments Co., Ltd., USA) of PA1012 and PA1012/PDP (APDP) were executed by attenuated total reflectance (ATR) technique at room temperature. The scanning scope is from 4000 to 400 cm^{-1} and the resolution is 0.5 cm^{-1}.

Thermal analysis for all samples were performed on a differential scanning calorimeter (DSC, TA Q20, TA Instruments, USA) under N_2 atmosphere. Firstly, the samples were heated to 230 °C at a heating rate of 20 °C·min^{-1} and held for 3 min to remove thermal history. Then, the samples were cooled to –20 °C at a cooling rate of 5 °C·min^{-1} and kept for 1 min. Finally, heated to 230 °C at 20 °C·min^{-1}.

The dynamic mechanical properties of all samples were tested using a dynamic mechanical analyzer (DMA, TA800, TA Instruments, USA) under liquid nitrogen conditions. Before the dynamic mechanical properties test, the splines of PA1012 and their composites (60×10×4 mm) were dried in a vacuum drying oven at 85 °C, and then the splines were heated from –50 to 150 °C at a heating rate of 5 °C·min^{-1} and a frequency of 1 Hz in a double-cantilever mode.

Tensile tests of all samples were measured with the electronic universal materials testing machine (GTM8050S, Xieqiang Instrument Manufacturing (Shanghai) Co., Ltd., China) at the stretching rate of 10 mm·min^{-1}. The notched impact strength was tested on XJC-25ZD (Chengde precision testing machine Co., Ltd., China) cantilever beam notch impact testing machine at the temperature of 25 °C. An impact energy of 2.75 J and impact speed of 3.5 m·s^{-1} was used. Before the impact test, the notch of 2 mm was made through the notch prototype (JJ-TEST, Chengde Jinjian testing instrument Co., Ltd., China).

Scanning electron microscopy (SEM, ZEISS EVO18, Carl Zeiss AG Co., Ltd., Germany) was operated at 10 kV to observe the morphology of the notched impact surface. Before SEM observation, the section of the notched impact sample is sprayed with gold.

3. Results and discussion

3.1. NMR analysis of acetylated PDP (APDP)

Figure 3 shows the ^1H NMR and ^{13}C NMR spectra of the PDP and APDP. It can be seen from Figure 3a the chemical shift of ^1H in the benzene ring is in the scope of 6.7–7.3 ppm. The chemical shift of ^1H in the pentadecyl long carbon chain lies in the range of

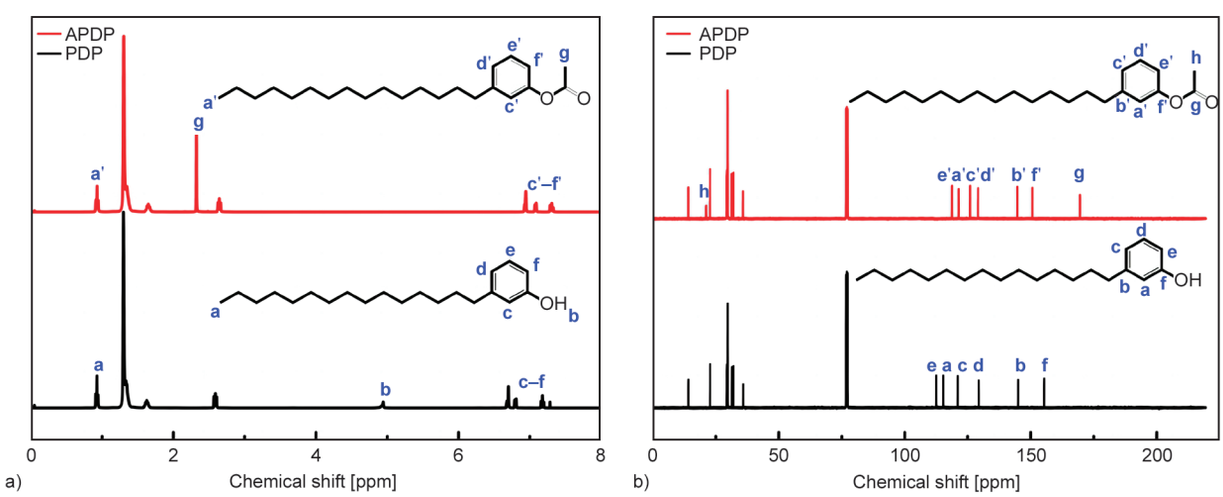

Figure 3. ^1H NMR (a) and ^{13}C NMR (b) spectra of neat PDP and APDP.

0.8–2.6 ppm. The chemical shift of ^{1}H from the phenol hydroxyl group is near 4.92 ppm. After PDP was acetylated, a chemical shift of ^{1}H from the phenol hydroxyl group couldn't be observed, and a new ^{1}H chemical shift of 2.28 ppm from $–CH_3$ from the ester group appeared, showing that the phenol hydroxyl group had been successfully acetylated. Furthermore, the typical ^{13}C NMR spectra from pristine PDP and APDP are shown in Figure 3b. Compared to the pristine PDP, the new signal at the chemical shifts of ^{13}C at 20.3 and 169 ppm can be observed, which should be assigned to the **h** ^{13}C and **g** ^{13}C in APDP, respectively, conforming again APDP that has been prepared. Moreover, after acetylation of PDP, the chemical shifts of ^{13}C at location **a–f** shifted. It is well known that the greater the electronegativity of substituents, the lower the chemical shift [20].

3.2. FTIR analysis

As shown in Figure 4a, the spectrum of APDP is quite similar to neat PDP, apart from the appearance of another peak at around 1758 and 1204 cm^{-1}, which are associated with the stretching vibration of C=O and C–O bond in the ester group from APDP. In addition, none of the characteristic absorption peaks at 3363 and 1265 cm^{-1} contributed by phenol hydroxyl groups from the PDP can be checked in the FTIR spectra of APDP. These distinguishing features proved that the acetylation of PDP was successful.

FTIR of PA1012/PDP and PA1012/APDP composites are shown in Figure 4b. As can be seen from Figure 4b, the IR absorption peak at 3300 cm^{-1} is resulted from N–H stretching vibration of the PA1012 molecular structure. The IR absorption peak at 1540 cm^{-1} (amide II) and 1636 cm^{-1} (amide I) are associated with N–H bending vibration ($\delta_{N–H}$) and C=O stretching vibration ($\nu_{C=O}$), respectively. With the addition of PDP into PA1012, the bending vibration absorption peak of the N–H bond of PA1012 shifts from 1542 to 1546 cm^{-1} in Figure 4c, meaning that an intermolecular hydrogen bond forms between PA1012 and PDP. Due to the substitution of some hydroxyl groups in PDP after acetylation modification, the characteristic peak of the N–H bond in the amide II band in composites did not move, which may reduce the hydrogen bond interaction between APDP and PA1012.

3.3. Crystallization and melting behavior

The crystallization and melting behavior may be altered after the incorporation of PDP or APDP, which will change matrix mechanical performance. DSC test results are recorded in Figure 5. As can be seen from Figure 5a, PDP has a sharp exothermic peak at 26.2 °C, and neat PA1012 has an obvious crystallization peak at around 163.8 °C. The crystallization peak temperature of PA1012 shifted to a lower temperature with increasing of PDP content, indicating that the hydrogen bonding interactions impede the motion of PA1012 molecular chains and inhibit the crystallization behavior during the cooling process from the melt so that the crystallization temperature (T_c) decreased [21]. After adding 20 wt% APDP, the crystallization peak temperature of PA1012 also shifts to a lower temperature, and the shift is lower than that of PA1012 with the same PDP content. This is due to the fact that APDP acts only as a plasticizer and can reduce entanglement between molecular chains, thereby increasing their volume and mobility. It can be seen that the hydrogen bond interaction plays a key role in the crystallization of PA1012.

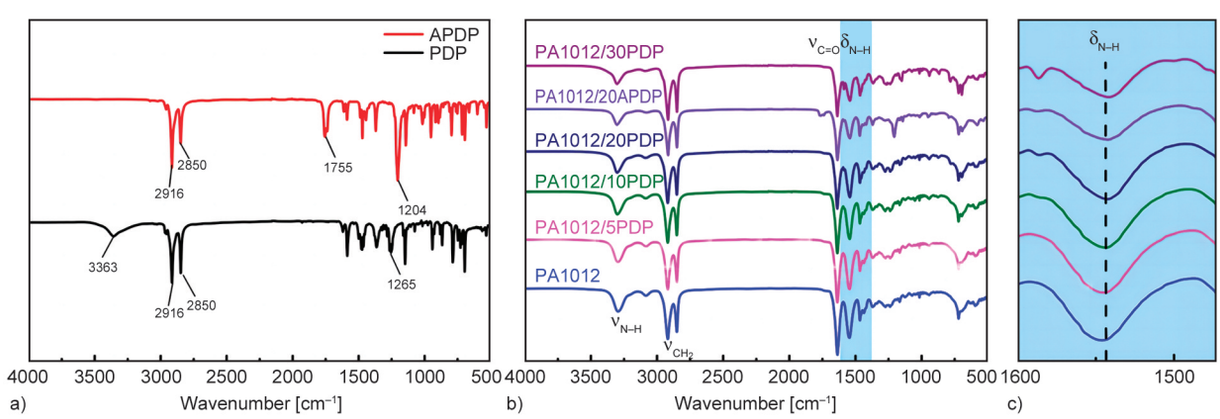

Figure 4. a) ATR-IR spectra of PDP, APDP; b) PA1012 and its composites in the wave number region of 4000–500 cm^{-1}; c) bending vibration of N–H bond of PA1012 and its composites.

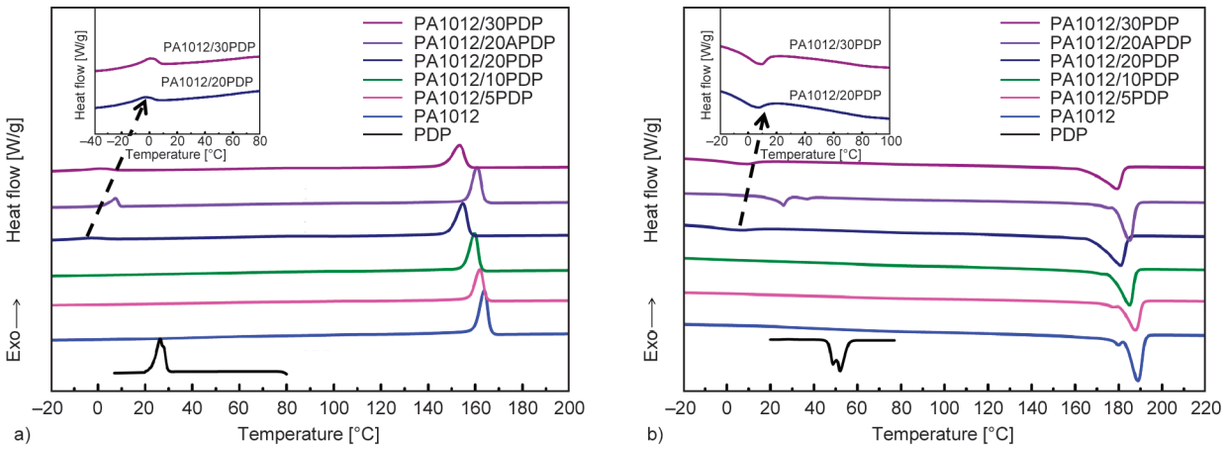

Figure 5. a) Crystallization and b) melting curves of PA1012, PDP, PA1012/PDP and PA1012/20APDP composites.

When the content of PDP and APDP was 20 wt%, a new exothermic peak below the crystallization temperature of pure PDP can be observed, which may be caused by limited crystallization of the alkyl chain in PDP and APDP [22]. Similar characteristics are also exhibited for the melting process as shown in Figure 5b, and melting peak temperature PA1012 gradually reduces with increasing PDP and APDP content. Generally, the melting temperature is closely related to the thickness of the crystals. So, the reduced melting temperature of PA1012 implies that the lamellar thickness of PA1012 decreases with the incorporation of PDP and APDP, respectively [23]. Meanwhile, a new endothermic below the melting temperature of neat PDP can also be detected in the case of more than 20 wt% PDP and APDP content, respectively. This is attributed to the melting process of the crystalline phase of their alkyl chain [24].

3.4. The impact strength enhancement and mechanism analysis

Figure 6a shows the typical stress-strain behavior of PA1012 with increasing PDP and APDP. Obviously, the addition of PDP and APDP significantly affects the tensile properties of PA1012 and its strain increases with rising of PDP content. Additionally, the effect of APDP on the strain of PA1012 is far less than that of PDP under their same addition amount. The main reason is that the addition of PDP to PA1012 not only causes an increase in flexibility and extensibility of the PA1012 but also forms hydrogen bond interaction with PA1012. Besides, Figure 6a

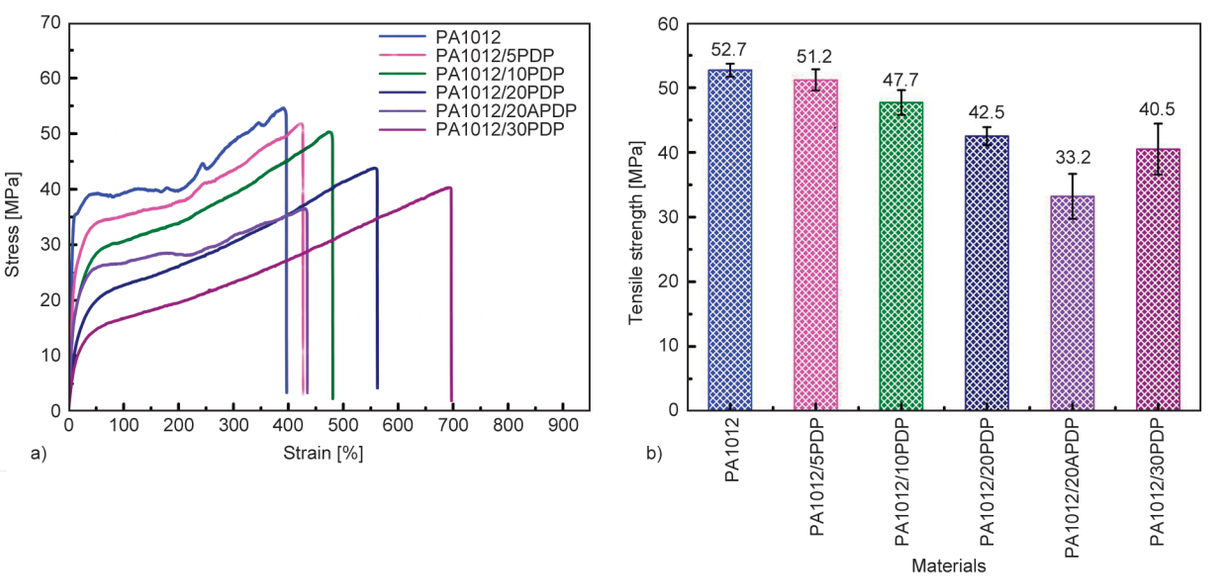

Figure 6. The mechanical properties for neat PA1012 and its composites. a) Stress-strain curves for all the materials; b) tensile strength.

also shows that the yield point of the composite disappeared when the content of PDP reached 20 wt%, indicating the occurrence of the brittle-ductile transition [25]. Moreover, the elongation at break was 690% for PA1012/PDP composites at 30 wt% of PDP and about 1.7 times higher than those of neat PA1012.

Figure 6b shows that the tensile strength changed with PDP concentration. It can be seen from Figure 6b that the tensile strength of PA1012 drops from 52.7 to 51.2, 47.7, 42.5 and 40.5 MPa with increasing PDP concentration. It is worth noting that the tensile strength of PA1012/20APDP composites is only 33.2 MPa, which is not only lower than that of PA1012/20PDP but also PA1012/30PDP. It was extremely encouraging to note that the toughening of PA1012 by PDP was not accompanied by a drastic reduction in tensile strength. This was because the strong intermolecular hydrogen bonding between PA1012 and PDP led to the enhancement of interfacial adhesion [26]. These results also show the hydrogen bonding interaction between PA1012 and PDP plays an important role, but the APDP maybe only play plasticization effects.

Figure 7 shows the relationship between the content of PDP and APDP and the notch impact strength. It's worth noting the PDP has significant effects on the impact strength. The impact strength of PA1012 ascends firstly and then descends with increasing of PDP content. Particularly, the notch impact strength reaches to the maximum value of 70.6 kJ·m^{-2} and is more than 7 times higher than that of the neat PA1012 when the PDP content is 20 wt%. Correspondingly, the addition of 20 wt% APDP only improved the notch impact strength of PA1012 by 2.3 times to 22.8 kJ·m^{-2}. Here, the impact strength of the PA1012/20PDP composite is higher than that of PA1012/20APDP, mainly due to the destruction and reconstruction of stronger H-bonding interaction in the PA1012/PDP system. In addition, the plasticization of PDP and APDP will promote the free movement and arrangement of PA1012 chains. Increased impact toughness of PA1012 [27, 28].

Figure 8 shows the effect of PDP and APDP on the storage modulus and tan δ as a function of the temperature of PA1012. As expected, the data of storage modulus, shown in Figure 8a, for each sample was decreased with increasing temperature. According to Karsli and Aytac [29], this phenomenon is explained by an increase in PA1012 chains mobility. The storage modulus of the PA1012/PDP composites with various contents of PDP at low temperatures was higher than neat PA1012. However, as the temperature is

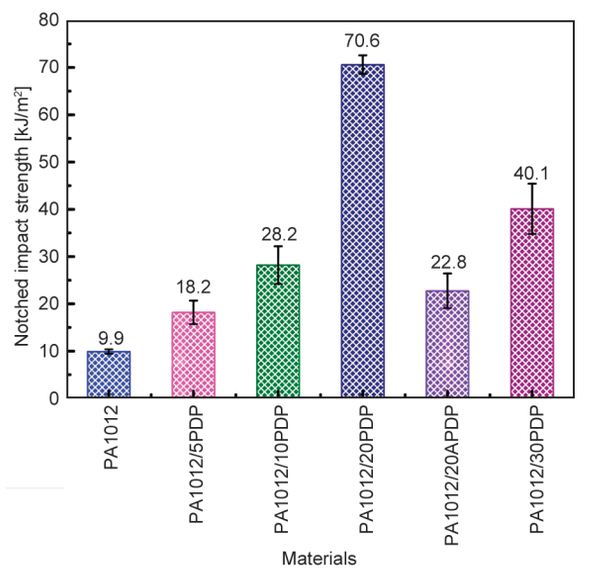

Figure 7. Impact toughness of PA1012 and its composites.

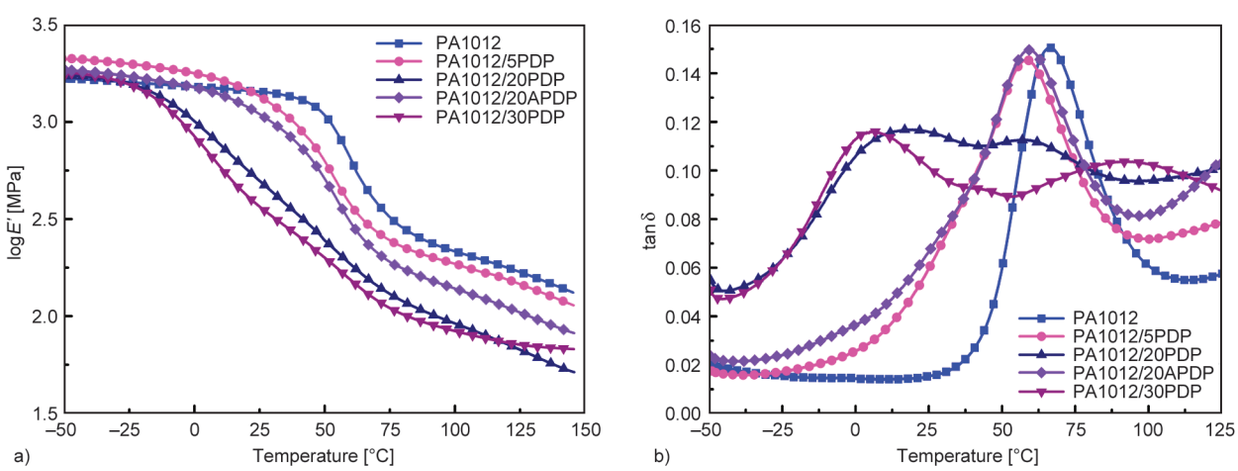

Figure 8. DMA analysis of PA1012 and their composites a) storage modulus (E'), b) tan δ.

increased, the storage modulus of all the composites became lower than neat PA1012 and dependent on the PDP weight fraction. That is, the higher the content of PDP, the more significant the plasticizing effect on PA1012, the larger the free volume of PA1012 molecular chain, and the easier the molecular movement.

In thermoplastics, the loss tangent (tan δ) value of a polymer reaches a maximum when the polymer is heated up to the glass transition temperature [29]. As can be seen from Figure 8b, the glass transition temperature (T_g) moves towards lower temperatures with increasing PDP content in PA1012/PDP composites. It is well known that the T_g of the matrix depends on the free volume of the polymer [30]. Here, the addition of PDP into PA1012 destroys the hydrogen bonding interaction resulting from PA1012 itself to some extent and obviously enhances chain mobility by increasing the free volume [31]. In addition, the formation of hydrogen bonding between PA1012 and PDP is responsible for a reduction in the intermolecular interactions between the chains and results in a sharp decrease in T_g [32]. Nevertheless, the most notable fact related to Figure 8b is that the PA1012/20APDP composites showed higher T_g shifts compared to the corresponding PA1012/20PDP composites. It is well known that the low tan δ indicates hard chain segment motion because it needs to overcome high friction. This high friction is caused by strong intermolecular interaction. Thus the decrease of the tan δ peak values indicates that the intermolecular interaction in PA1012/PDP system, again suggesting that the PA1012 has stronger interaction with PDP compared to APDP [33, 34].

3.5. Scanning electron microscopic analysis

To better understand the morphology evolution of the brittle to ductile transition of samples after mixing different content PDP and APDP into PA1012. Scanning electron microscopy images of the samples are shown in Figure 9. Figure 9a corresponds to the fracture surfaces of neat PA1012. The smooth and lesser fluctuation surface morphology for neat PA1012 indicates it has lower impact strength due to a lack

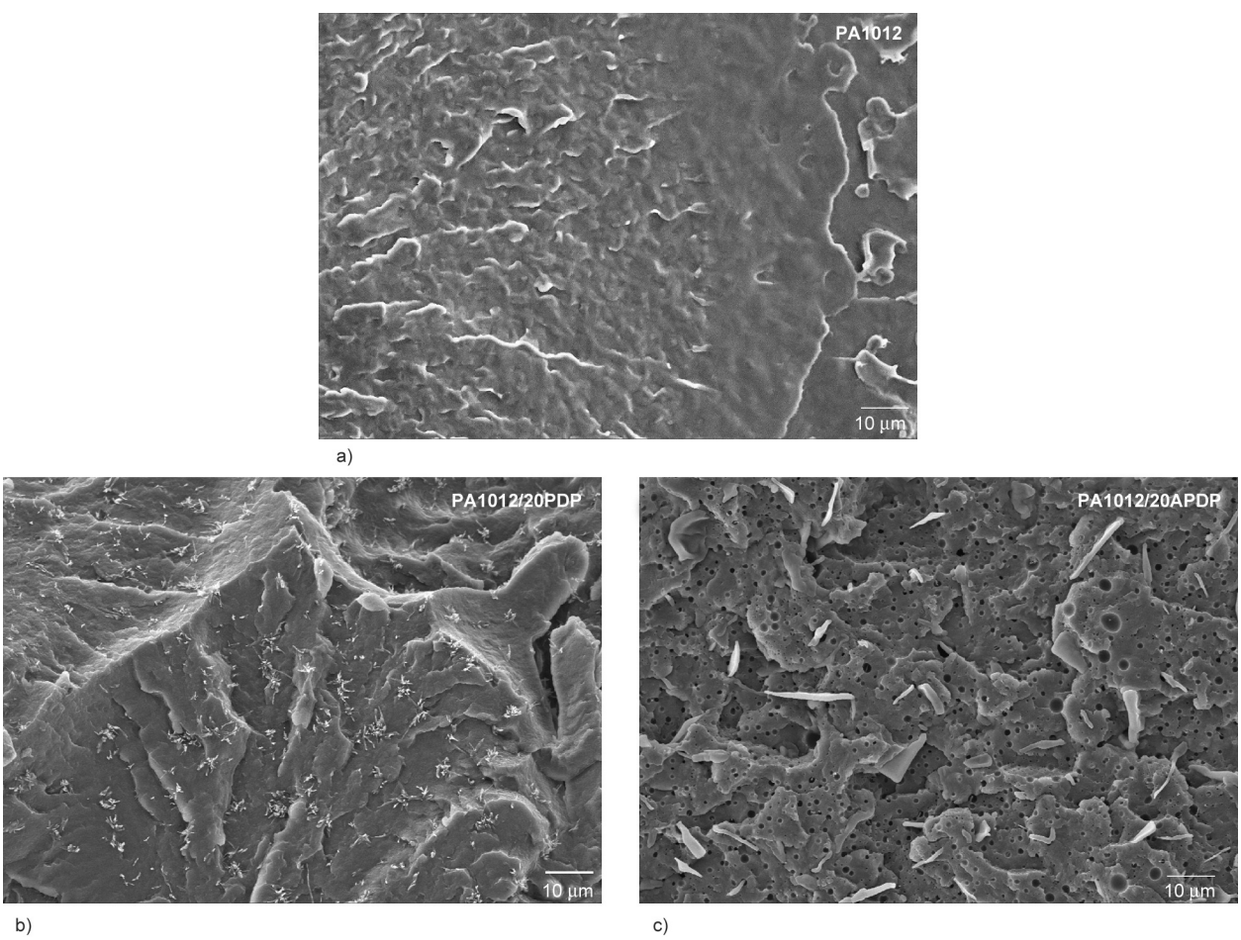

Figure 9. The SEM images (×1000) of fracture surface for a) the neat PA1012; b) composites with 20 wt% PDP content; c) composites with 20 wt% APDP content.

of absorbing energy, which belongs to the typical brittle fracture characteristics. In addition, the microcrack of the surface of neat PA1012 is almost locates on the same layer and diffuses towards the same direction. However, after adding PDP and APDP, the morphology of the fracture surface changed significantly. PA1012/20PDP composites micrograph reveals a fracture surface with a very irregular massive crack and rough appearance in Figure 9b, showing the resistance of crack propagation improves and the typical ductile behavior occurs. It is found that the PDP small molecules with uniform distribution appeared on the surface. However, in contrast to the PA1012/20PDP composites, the fracture surface of the PA1012/20APDP composites was relatively flat, and there was a large area of shear yield and holes, showing obvious ductile fracture behavior, too. A similar phenomenon has been observed in the lignin/polyamide 6 blends by Sallem-Idrissi *et al.* [35]. The voids observed in the SEM image of PA1012/ APDP should be APDP phase.

4. Conclusions

In this work, PA1012/PDP composites were prepared by a simple melting blending method and the impact toughness was optimized substantially. The H-bonding toughening effects on PA1012 systems are explained by acetylating modified PDP. An analysis of the acetylated PDP with NMR revealed that the PDP has been successfully modified. The intermolecular H-bonds between PA1012, PDP and APDP were characterized by FTIR, respectively. The crystallization behavior is also reflected by the significantly lowered crystallization and melting temperature of the PA1012 matrix in the composites than neat PA1012. However, the tensile strength of PA1012 composites becomes smaller with the increase in PDP and APDP content. SEM study shows that the morphology of the impact section is obvious ductile fracture for the composites with 20 wt% of PDP and APDP due to the existence of the PDP and APDP. This work suggests a facile strategy for enhancing the impact toughness of polyamide via H-bonding interaction. This is helpful to expand the application prospect of semi crystalline polyamide materials.

Acknowledgements

We appreciate the funding support from the Key Natural Science Foundation of, the open project of State Key Laboratory of High-efficiency Utilization of Coal and Green Chemical Engineering and First-class discipline construction (Chemical Engineering and Technology) in Ningxia University (Grant/Award Numbers are 2022AAC02017, 2019-KF-17 and NXYLXK2017A04).

References

[1] Muthuraj R., Hajee M., Horrocks A. R., Kandola B. K.: Biopolymer blends from hardwood lignin and bio-polyamides: Compatibility and miscibility. International Journal of Biological Macromolecules, **132**, 439–450 (2019). https://doi.org/10.1016/j.ijbiomac.2019.03.142

[2] Liu X., Wang Y., Wang Z., Cavallo D., Müller A. J., Zhu P., Zhao Y., Dong X., Wang D.: The origin of memory effects in the crystallization of polyamides: Role of hydrogen bonding. Polymer, **188**, 122117 (2020). https://doi.org/10.1016/j.polymer.2019.122117

[3] Gao X., Zhang D., Wen X., Qi S., Su Y., Dong X.: Fused deposition modeling with polyamide 1012. Rapid Prototyping Journal, **25**, 1145–1154 (2019). https://doi.org/10.1108/RPJ-09-2018-0258

[4] Song J., Liu J., Zhang Y., Chen L., Zhong Y., Yang W.: Basalt fibre-reinforced PA1012 composites: Morphology, mechanical properties, crystallization behaviours, structure and water contact angle. Journal of Composite Materials, **49**, 415–424 (2015). https://doi.org/10.1177/0021998313519484

[5] Li X., Wang L., Wang D., Müller A. J., Dong X.: Competition between chain extension and crosslinking in polyamide 1012 during high-temperature thermal treatments as revealed by successive self-nucleation and annealing fractionation. Macromolecules, **54**, 7552–7563 (2021). https://doi.org/10.1021/acs.macromol.1c01252

[6] Yang R., Chen F., Iqbal M. I., Wang L., Zhang C., Bao H.: The effect of carbon fibre reinforced on polyamide 1012. Journal of Fiber Bioengineering and Informatics, **11**, 41–47 (2018). https://doi.org/10.3993/jfbim00279

[7] Zhou C., Zhu P., Liu X., Dong X., Wang D.: The toughening mechanism of core-shell particles by the interface interaction and crystalline transition in polyamide 1012. Composites Part B, **206**, 108539 (2021). https://doi.org/10.1016/j.compositesb.2020.108539

[8] Peng J., Qiao J., Zhang S., Wei G.: A novel impact modifier for nylon 6. Macromolecular Materials and Engineering, **287**, 867–870 (2002). https://doi.org/10.1002/mame.200290018

[9] Sharif N. F. A., Mohamad Z., Hassan A., Wahit M. U.: Novel epoxidized natural rubber toughened polyamide 6/halloysite nanotubes nanocomposites. Journal of Polymer Research, **19**, 9749 (2012). https://doi.org/10.1007/s10965-011-9749-5

[10] Zhang Y., Wang Y., Xu Y., Liu X., Guo W.: Modification of biobased polyamide 56 to achieve ultra-toughening. Polymer-Plastics Technology and Materials, **60**, 1585–1604 (2021). https://doi.org/10.1080/25740881.2021.1924198

[11] Bai J., Yuan S., Shen F., Zhang B., Chua C. K., Zhou K., Wei J.: Toughening of polyamide 11 with carbon nanotubes for additive manufacturing. Virtual and Physical Prototyping, **12**, 235–240 (2017). https://doi.org/10.1080/17452759.2017.1315146

[12] Shi J., Wang Y., Gao Y., Bai H.: Effects of coupling agents on the impact fracture behaviors of T-ZnOw/PA6 composites. Composites Science and Technology, **68**, 1338–1347 (2008). https://doi.org/10.1016/j.compscitech.2007.12.004

[13] Xu M., Lu J., Qiao Y., Wei L., Liu T., Lee P. C., Zhao L., Park C. B.: Toughening mechanism of long chain branched polyamide 6. Materials Design, **196**, 109173 (2020). https://doi.org/10.1016/j.matdes.2020.109173

[14] Corté L., Leibler L.: A model for toughening of semicrystalline polymers. Macromolecules, **40**, 5606–5611 (2007). https://doi.org/10.1021/ma0706935

[15] Zhang S-L., Wang G-B., Jiang Z-H., Wang D., Ma R-T., Wu Z-W.: Impact properties, phase structure, compatibility, and fracture morphology of polyamide-1010/thermoplastic poly(ester urethane) elastomer blends. Journal Polymer Science Part B: Polymer Physics, **43**, 1177–1185 (2005). https://doi.org/10.1002/polb.20410

[16] Li L., Liu S., Liu R., Geng C., Hu Z.: Preparation and characterization of hydrophilic wetting-modified polyamide fibers. Advances in Polymer Science, **2020**, 8475497 (2020). https://doi.org/10.1155/2020/8475497

[17] Reusch R. N., Sadoff H. L.: 5-n-alkylresorcinols from encysting *Azotobacter vinelandii*: Isolation and characterization. Journal of Bacteriology, **139**, 448–453 (1979). https://doi.org/10.1128/jb.139.2.448-453.1979

[18] Kubo I., Komatsu S., Ochi M.: Molluscicides from the cashew *Anacardium occidentale* and their large-scale isolation. Journal of Agricultural and Food Chemistry, **34**, 970–973 (1986). https://doi.org/10.1021/jf00072a010

[19] Cieślik-Boczula K., Koll A.: The effect of 3-pentadecylphenol on DPPC bilayers ATR-IR and ^{31}P NMR studies. Biophysical Chemistry, **140**, 51–56 (2009). https://doi.org/10.1016/j.bpc.2008.11.009

[20] Zhang X., Wang J., Xu Y-Z.: Systematic assignment of NMR spectra of 5-substituted-4-thiopyrimidine nucleosides. Magnetic Resonance Chemistry, **51**, 523–529 (2013). https://doi.org/10.1002/mrc.3980

[21] Zheng X., Lin Q., Jiang P., Li Y., Li J.: Ionic liquids incorporating polyamide 6: Miscibility and physical properties. Polymers, **10**, 562–581 (2018). https://doi.org/10.3390/polym10050562

[22] Sun X., Luo F., Yan D.: The preparation of chain branching PLLA by intermolecular hydrogen bonding with 3-pentadecylphenol and its crystallization, relaxation behavior and thermal stability. Journal of Polymer Research, **26**, 81 (2019). https://doi.org/10.1007/s10965-019-1729-1

[23] Wang L-L., Dong X., Wang X-R., Zhu G-Y., Li H-Q., Wang D-J.: High performance long chain polyamide/calcium silicate whisker nanocomposites and the effective reinforcement mechanism. Chinese Journal of Polymer Science, **34**, 991–1000 (2016). https://doi.org/10.1007/s10118-016-1812-6

[24] Zeng W., Wang J., Feng Z., Dong J-Y., Yan S.: Morphologies of long chain branched isotactic polypropylene crystallized from melt. Colloid Polymer Science, **284**, 322–326 (2005). https://doi.org/10.1007/s00396-005-1371-9

[25] Wang L., Dong X., Huang M., Müller A. J., Wang D.: The effect of microstructural evolution during deformation on the post-yielding behavior of self-associated polyamide blends. Polymer, **117**, 231–242 (2017). https://doi.org/10.1016/j.polymer.2017.04.038

[26] Chen L., Qin Y., Wang X., Zhao X., Wang F.: Plasticizing while toughening and reinforcing poly(propylene carbonate) using low molecular weight urethane: Role of hydrogen-bonding interaction. Polymer, **52**, 4873–4880 (2011). https://doi.org/10.1016/j.polymer.2011.08.025

[27] Song P., Xu Z., Guo Q.: Bioinspired strategy to reinforce PVA with improved toughness and thermal properties *via* hydrogen-bond self-assembly. ACS Macro Letters, **2**, 1100–1104 (2013). https://doi.org/10.1021/mz4005265

[28] Caillol S.: Cardanol: A promising building block for biobased polymers and additives. Current Opinion in Green and Sustainable Chemistry, **14**, 26–32 (2018). https://doi.org/10.1016/j.cogsc.2018.05.002

[29] Karsli N. G., Aytac A.: Tensile and thermomechanical properties of short carbon fiber reinforced polyamide 6 composites. Composites Part B: Engineering, **51**, 270–275 (2013). https://doi.org/10.1016/j.compositesb.2013.03.023

[30] Rangari V. K., Yousuf M., Jeelani S., Pulikkathara M. X., Khabashesku V. N.: Alignment of carbon nanotubes and reinforcing effects in nylon-6 polymer composite fibers. Nanotechnology, **19**, 245703 (2008). https://doi.org/10.1088/0957-4484/19/24/245703

[31] Baji A., Mai Y-W., Wong S-C., Abtahi M., Du X.: Mechanical behavior of self-assembled carbon nanotube reinforced nylon 6,6 fibers. Composites Science and Technology, **70**, 1401–1409 (2010). https://doi.org/10.1016/j.compscitech.2010.04.020

[32] Feldman D., Banu D.: Interactions in poly(vinyl chloride)–lignin blends. Journal of Adhesion Science and Technology, **17**, 2065–2083 (2003). https://doi.org/10.1163/156856103322584218

[33] Podolyák B., Kun D., Renner K., Pukánszky B.: Hydrogen bonding interactions in poly(ethylene-*co*-vinyl alcohol)/lignin blends. International Journal of Biological Macromolecules, **107**, 1203–1211 (2018). https://doi.org/10.1016/j.ijbiomac.2017.09.098

[34] Li B., Pang Y., Fan C., Gao J., Wang X., Zhang C., Liu X.: Influence of hydrogen-bonding interaction introduced by filled oligomer on bulk properties of blended polyimide films. Journal of Applied Polymer Science, **131**, 1–9 (2014). https://doi.org/10.1002/app.40498

[35] Sallem-Idrissi N., Sclavons M., Debecker D. P., Devaux J.: Miscible raw lignin/nylon 6 blends: Thermal and mechanical performances. Journal of Applied Polymer Science, **133**, 42963 (2016). https://doi.org/10.1002/app.42963